



Journal of GeoSpace Science

ISSN-xxx-xxx

Open Access Biannual Research Journal publish by Institute of Space and Planetary Astrophysics

Journal home page: <http://www.jogss.org/>

Variation in Aerosol Optical Depth and its Impact on Longwave Radiative Properties in Northern Areas of Pakistan

Samina Bibi¹, Khan Alam^{*1}, Humera Bibi¹, Hidayat Ullah Khan¹, Bibi Safia Haq²

¹Department of Physics, University of Peshawar, Peshawar 25120, Pakistan

²Jinnah College for Women, Department of Physics, University of Peshawar, Peshawar, Pakistan

ARTICLE INFO

Article history:

Received 31 August 2015

Received in revised form 12

September 2015

Accepted 15 September 2015

Available online 24 September 2015

Keywords: aerosol optical depth, aerosol radiative fluxes, moderate imaging spectroradiometer, hybrid single particle lagrangian integrated trajectory and northern Pakistan

ABSTRACT

Annual and seasonal variations in aerosol optical depth (AOD) at a wavelength of 550nm have been investigated using MODIS (Moderate Imaging Spectroradiometer). In addition, average Aerosol Radiative Fluxes (ARF) have been calculated for the Long Wavelength (LW) clear sky at the Top Of the Atmosphere (TOA), the earth's surface (SRF), and within the atmosphere (ATM) using the Earth's Radiant Energy System (CERES) data over Peshawar, Dera Ismail Khan (D I Khan), Swat and Chitral during December 2002 – February 2005. The results have revealed that the annual mean AOD at 550 nm were 0.37 ± 0.13 , 0.73 ± 0.37 , 0.31 ± 0.10 and 0.22 ± 0.09 over Peshawar, D I Khan, Swat and Chitral respectively. Seasonal variations revealed that summer, winter, pre-monsoon and post-monsoon AODs were higher over D I Khan and Peshawar while lower over Swat and Chitral. The monthly average ARF variation at the TOA, SRF and ATM during clear-sky days have been calculated. ARF computed from CERES model has yielded negative value (-102 W/m^2) at the SRF and positive value (259 W/m^2) at the TOA with a high value of ATM (399 W/m^2) leading to heating effect over D I Khan during the study period. This value (399 W/m^2) for atmospheric forcing was highest amongst those recorded for other sites aforementioned. Further, AODs compared with ARF at the SRF, TOA and ATM over all the sites, and was found reasonable relationship within ATM over the sites investigated. The Hybrid Single Particle Lagrangian Integrated Trajectory (HYSPLIT) model was used for back trajectories assessment. In addition to local (Baluchistan Punjab and Azad Kashmir) air masses, the long range transported air masses arrive at the study sites from Iran, Turkmenistan, India and Afghanistan.

© 2015 JOGSS Publisher All rights reserved.

To Cite This Article: Samina Bibi; Khan Alam; Humera Bibi; Hayat Ullah Khan and Bibi Safia Haq., Variation in Aerosol Optical Depth and its Impact on Longwave Radiative Properties in Northern Areas of Pakistan., *Jour. of GeoSpace Science*, (1), 28-43, 2015

INTRODUCTION

Under clear sky conditions the Aerosol Radiative Flux (ARF) is the difference between incoming and outgoing solar flux in the presence and absence of aerosols. The radiative flux within the atmosphere (ATM) with aerosol can be obtained from either satellite data or model calculation, using "received input data" while the "flux", in the absence of aerosol, from the model observation (Lesins et al, 1999). Radiative flux, measured in W/m^2 , can be described as the magnitude of power in the form of photons or other elementary particles emitted through a given region. When restrained

Corresponding Author: Khan Alam, Department of Physics, University of Peshawar, Peshawar 25120, Pakistan.

Tel: +92-91-9216727; E-mail: khalalamso@gmail.com

to the infrared spectrum, radiative flux acts as heat flux, and becomes irradiance when incident upon a surface (Pollack et al., 1993).

Radiative flux is classified into two types – (i) Short Wave (SW) radiative flux and (ii) Long Wave (LW) radiative flux. Both of fluxes are the result of specular and diffuse reflection of infrared waves. Short wave radiation has a profound impact on certain biophysical processes such as photosynthesis and land surface energy budget and long wave radiative flux is the product of both down welling as well infrared energy as well as emission by the surface (Pawar et al., 2012).

Aerosol effect on atmospheric radiative fluxes precedes a forcing function that can change the climate in significant ways. ARF is a major observed climate change of the past century and in predicting future climate (Russell et al., 1999). The SW and LW radiative fluxes are critical components of energy balance, and play a vital role for understanding the weather and climate within the atmosphere (Karatz et al., 2000). Aerosols exert Direct Radiative Effects (DRE) due on scattering and absorption of sunlight (Satheesh and Ramanathan, 2000). Aerosol scattering is the dominant aerosol forcing that leads to the cooling of the atmosphere. Absorption of solar radiation by aerosols leads to the warming of the surrounding, changing thereby the temperature and strength of convection (Chou et al., 2005). The magnitude of DRE depends on the relative proportion of natural and anthropogenic aerosols constituents which have manifest characteristics and size assessment (Griggs et al., 2002). The direct radiative forcing due to the biomass burning aerosols is a sensitive function of the size distribution of aerosol particles. The DRE due to anthropogenic and natural aerosols is define as the effect of these aerosols on the radiative fluxes and the change in radiative flux due to only anthropogenic aerosol can be termed as aerosol direct radiative forcing (Chung et al., 2005).

(Chakraborty et al., 2010) studied the impact of absorbing aerosol on the simulation of climate over the Asian region in an atmospheric general circulation model and they show that, the absorbing aerosols increase short wave radiative heating of the lower troposphere and reduce the heat at the surface. Until now, few studies have been conducted on aerosol optical properties in Lahore and Karachi (Alam et al., 2011b), (Alam et al., 2012), (Alam et al., 2014a) and (Alam et al., 2014b). The radiative forcing in New Delhi was studied and increase in heating was observed at the top of the atmosphere (Pandithurai, 2008). The direct radiative forcing of Indian Ocean region during spring 1999 was reduced in atmosphere (Collins et al., 2002). (Qin et al., 2009) reported that the heating rate is increased over Tibetan Plateau (China). (Deepshikha et al., 2005) derived the dust absorbing efficiency over the north Indian Ocean on the bases of METEOSAT observation in the U-V visible and infra-red spectrum, and observed that the dust from desert areas of Arabian Peninsula was less absorbing than the one interacting with anthropogenic aerosols which provides strong evidence for occasional dust particles with black carbon.

(Menon et al., 2002) studied the climate effects of the black carbon aerosols in the East Asian monsoon region and found the phenomenon of northern drought/southern flooding occurred in summer during the past 50 years in China. Heating effects due to carbonaceous aerosols in the atmosphere went up in the Himalayan region accompanied by the weakening of the Hadley and polar circulations in the Northern Hemisphere (Zhang et al., 2009).

The present work analyzed the spatio-temporal variations in Aerosol Optical Depth (AOD), and Long Wave (LW) Aerosol Radiative Fluxes (ARF) at TOA, SRF and in ATM using Clouds and the Earth's Radiant Energy System (CERES) and Moderate Resolution Imaging Spectroradiometer (MODIS)

instruments data over Peshawar, D I Khan, Swat and Chitral for the period December 2002 – February 2005. The relationship between ARFs and AODs has been examined. In order to investigate the origin of air mass back trajectory, the Hybrid Single Particle Lagrangian Integrated Trajectory (HYSPPLIT) has also been utilized.

2 Methodologies

2.1 Site description

Peshawar ($34^{\circ}01' N$, $71^{\circ}35' E$) covering area $1,257 \text{ km}^2$ with a population of approximately 3,307,798. Peshawar has a semi-arid climate with very hot summers and mild winters. Winter begins in mid- November and ends in late march, while summer months are May to September. The mean maximum temperature during the hot summer is 40°C (104°F) and mean minimum temperature is 25°C (77°F). The mean minimum temperature in winter is 4°C (36°F) while maximum temperature is 18.5°C (50.5°F). The map of Khyber Pakhtunkhwa (KP) is shown in Figure 1 in which the study areas are shown. Peshawar is not a monsoon region, unlike other parts of Pakistan; however, rainfall occurs in both winter and summer. The sources of aerosol concentration over this site are Industrial emission and vehicular emission, road dust, smoke etc.



Fig.1: Map of Pakistan showing the study site

D I Khan ($31^{\circ}49' N$, $71^{\circ}55' E$) is located on the west bank of river Indus covering area $7,326 \text{ km}^2$ with a population of approximately 852,995. D I Khan has a hot desert climate with hot summers and mild winters. Precipitation mainly falls in two distinct periods, in the late winter and early spring from February to April, and in the monsoon in June and July. Emissions from sugar mills, textile mills, ghee mills, flour mills, and dates processing remains of blasting materials may increase in AOD concentrations over D I Khan.

Swat ($34^{\circ}01' N$, $71^{\circ}35' E$) upper valley of the Swat River is situated in the north of KP is enclosed by the sky-high mountains covering area is $5,337 \text{ km}^2$ having a population of about 2,161,000. The average temperature in the month of June is about 35°C and decreases to about 26°C in July and August with a little chance of rain. The average temperature in the month of January is about 11°C and decreases to about -2°C in July. It has two major seasons, summer season from May to August with high relative humidity and frequent rains and the dry season from April to May. Industries are not so developed by the time the site is in Swat, so the major sources of aerosols are soot from

wood stoves, burning coal, fuel and oil, emission from vehicle, atmospheric gases, road dust, etc., contribute to aerosol concentration.

Chital (35°50' N, 71°47' E) is a valley located in the extreme north of Pakistan with the larger part of Chital is covered with high mountains and hills covering area is 14,850km² having population of about 600,000. This town is at the foot of Turch Mir, the highest peak of Hindukush which is 25,289 feet high. Winter snowfall in the town can be quite heavy with an accumulation of up to two feet being quite common, at higher elevation snowfall can reach as high as 20 meters (70 ft). The weather is very cold during the winter.

2.2 Datasets and analyses (instrumentation)

In this study different datasets and their derived properties have been used. MODIS satellite is a key instrument that installed on the Terra (EOS AM) and Aqua (EOS PM) satellites which were launched in December 1999 and May 2002, respectively. Terra's orbit around the earth in the morning it passes from north to south across the equator, while Aqua passes south to north over the equator in the afternoon. MODIS uses 36 spectral bands with wavelengths ranged (0.41 μm -14.4 μm). MODIS instrument give a lot of information about meteorological, terrestrial, and coastal surroundings. It has (250-1km) spatial and (1-2) days temporal resolution, but for some parameters it also provides a spatial resolution of 10 km [18]. MODIS uses different methods for retrieval data over oceans [19] and over land [20] and for land it shows less accuracy [21]. The MOD08 AOD monthly data products from Terra level-3 AOD at wavelength 550nm with a spatial resolution of 1° × 1° km from December 2002 to February 2005 were utilized in this study. More information on retrieval of AOD data is available at website <http://modis-atmos.gsfc.nasa.gov>.

The Clouds and the Earth's Radiant Energy System (CERES) instruments fly on several National Aeronautics and Space Administration Earth Observing System (EOS) satellites starting in 1998 and now it is a key constituent of the Earth Observing System (EOS) program. The CERES broadband scanning radiometers are modified version of the Earth Radiation Budget Experiment (ERBE) radiometers [22]. CERES monitors infinitesimal changes in the Earth's energy balance, the difference between incoming and outgoing energy and determine the Earth's energy balance providing a long term record of this vital environmental parameters that will be reliable with those of its precursors. The CERES instruments also provide radiometric measurement of the Earth's atmosphere from three broadband channels. The CERES instrument is scanning Earth, helping to assure availability of measurement of the energy at TOA, at the SRF and at several selected levels within ATM [5]. CERES data provide TOA radiative fluxes with a factor of 2 to 3 less error than the ERBE data. In this study we have used CERES product having concurrent information of Clear-sky_TOA_LW_Flux and Clear-sky_Sfc_Net_LW_Flux-Mod_B for the study period. The detail on retrieval of ARF data is available at website <http://disc.sci.gsfc.nasa.gov/giovanni>.

NOAA HYSPLIT (National Oceanic and Atmospheric Administration Hybrid Single Particle Lagrangian Integrated Trajectory) model is used to calculate air mass trajectories, in specific backward and forward trajectories, with meteorological variables (ambient temperature, rainfall, relative humidity, solar radiation flux) [23]. In this study, we used NOAA HYSPLIT (National Oceanic and Atmospheric Administration Hybrid Single Particle Lagrangian Integrated Trajectory) model for back trajectories in order to investigate the source of air masses arriving the study sites. We run this model for 3-day time period (72 hours) through the website (<http://ready.arl.noaa.gov/HYSPLIT.php>).

3. Results and discussion

3.1 Annual and seasonal variations in AOD

In this study, we derived time series of monthly mean AOD values from MODIS at 550nm for the period of December 2002 - February 2005 and found that the monthly mean MODIS AOD values ranged from 0.21-1.62, 0.22-1.57, 0.19-0.58, and 0.08-0.42 over Peshawar, D I Khan, Swat and Chitral respectively. Figure 2(a-d) showed that the highest average AOD was observed in D I Khan (1.57), and the lowest in Chitral (0.08). Every year AOD attained annual peak in the month of July at all locations except Chitral. Annual and seasonal average AOD values and standard deviations retrieved by MODIS over Peshawar, D I Khan, Swat and Chitral during the study period was given in Table 1.

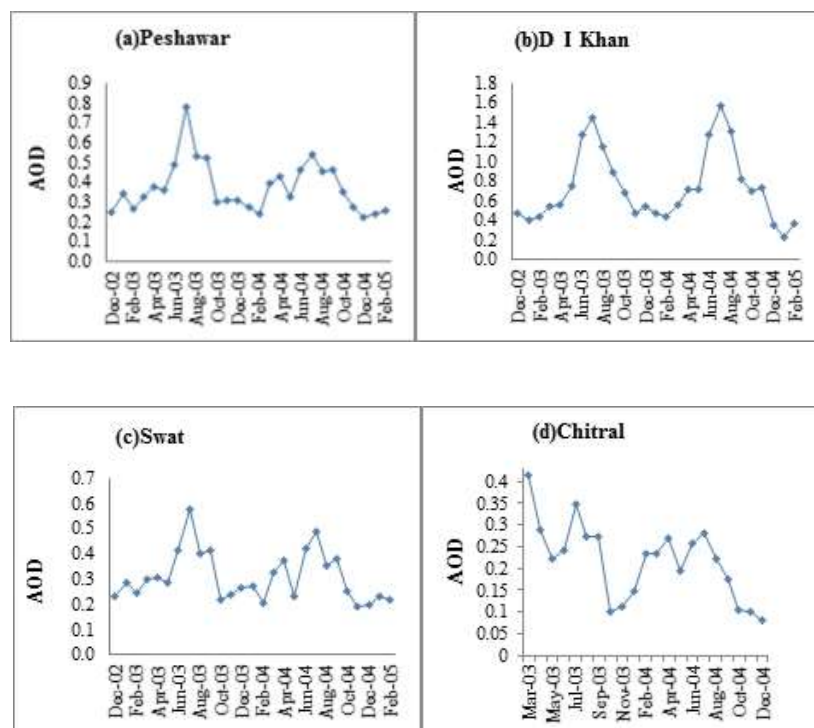


Fig. 2: Annual variations in AOD for the period (December 2002– February 2005) over Peshawar, D I Khan, Swat and Chitral.

Figure 2(a-d) showed that, for Peshawar, the maximum AOD value (0.78) was recorded during the month of July 2003; for D I Khan, the maximum AOD value (1.57) in July 2004; for Swat, the maximum AOD value of 0.58 was in June 2003; for Chitral, the maximum AOD value of 0.42 in March 2003.

A marked AOD maximum was observed in month July is due to the increase in temperature, absence of rain and harvesting of crops. The AOD value over Chitral was highest in March 2003. This increased AOD value in march is due to local air pollutants and strong wind erosion. Additionally the decrease in AOD values was observed from September to December for all sites which is due the cloud scavenging and rain wash out processes. (Jin et al., 2006) observed maximum AOD from May to June and the minimum from November to December over the Tibetan Plateau.

Table 1. Annual and seasonal means and standard deviations of AOD retrieved by MODIS at 550nm over Peshawar, D I Khan, Swat and Chitral during the study period

Sites	Annual	Winter	Summer	Pre-monsoon	Post-monsoon
Peshawar	0.37±0.13	0.26±0.04	0.56 ±0.13	0.37±0.04	0.38±0.09
D I Khan	0.73±0.37	0.41±0.09	1.34±0.17	0.64±0.10	0.71±0.14
Swat	0.31±0.10	0.24±0.03	0.46±0.07	0.30±0.05	0.28±0.09
Chitral	0.22±0.09	0.15±0.08	0.28±0.05	0.27±0.08	0.14±0.06

(Sarkar et al., 2006) reported that AOD from March started to increase and reaches a maximum value in June over India. (Alam et al., 2011b) found the same result that AOD increased from the month of March, reaching its maximum in July over Karachi. On the contrary AOD started to decrease in September and found the low value in December. Our results were also consistent to the ones found by (Metwally et al., 2010) using MODIS aerosol retrievals over Cairo (Egypt). We also carried out a seasonal average MODIS AOD over Peshawar, D I Khan, Swat and Chitral for the summer (June, July, August), winter seasons (December, January, February), pre-monsoon (March, April, may) and post-monsoon (September, October, November) for the period December 2002–February 2005.

MODIS retrieved AOD varies significantly over seasons. Figure 3(a-d) presented the average AOD values as a function of month, showing seasonal variations for the four selected cities with a high AOD value in July during the summer season in almost all regions. Similarly, high AOD values were obtained in the December during the winter season for all sites except Chitral because over Chitral for winter months not much data were available to make any precise observations. It was also evident from the Figure that summer AOD's were higher than winters. Figure 3(c-d) showed that AOD values in post monsoon were high while low in pre-monsoon over Peshawar and D I Khan. In contrast AOD values in pre-monsoon were high while low in post-monsoon over Swat and Chitral. (Ranjan et al., 2007) reported that in summer, higher humidity indicates higher AOD values. (Balakrishnaiah et al., 2012) observed high AODs values over Pune, Visakhapatnam and Hyderabad during the summer season using MODIS satellite data. (Tripathi et al., 2005) recorded maximum AODs values during the summer months retrieved from MODIS over Kanpur. (Li et al, 2003) used the MODIS data to analyze the seasonal variations of AOD in eastern China, and found the higher value of AOD in summer due to human activities and Asian dust. In terrestrial regions of China, the regional monthly average AOD values were analyzed from MODIS which showed higher values of AOD in summer and lower in winter (wang et al, 2008). (Papadimas et al., 2008) recorded high precipitation rate in winter which causes removal of atmospheric aerosols and a lower value of AOD during this season was observed. (Chen et al. 2010) observed the seasonal variability with a higher AOD level in summer and a lower AOD level in winter over Southern Ontari (Canada). Similarly, (Singh et al., 2010) found that the AOD was higher in summer season than in winter season for different areas of India. (Alam et al., 2014a) analyzed the retrieval of MODIS AOD over Lahore and noted high AOD values during post-monsoon than pre-monsoon. (Choudary et al., 2012) examined the aerosol concentrations over Kanpur (India) and that fond that AOD data increases during the

pre-monsoon months because dust storms were common in the Indo Gangetic Plain. Using MODIS data earlier researchers (Kalita et al., 2011) and (Pathak et al., 2013) have reported that highest fire activities in the region take place during pre-monsoon. (Kharol et al., 2008) have also attributed enhanced fire activities peaking in pre-monsoon over North-East India to observed high AOD.

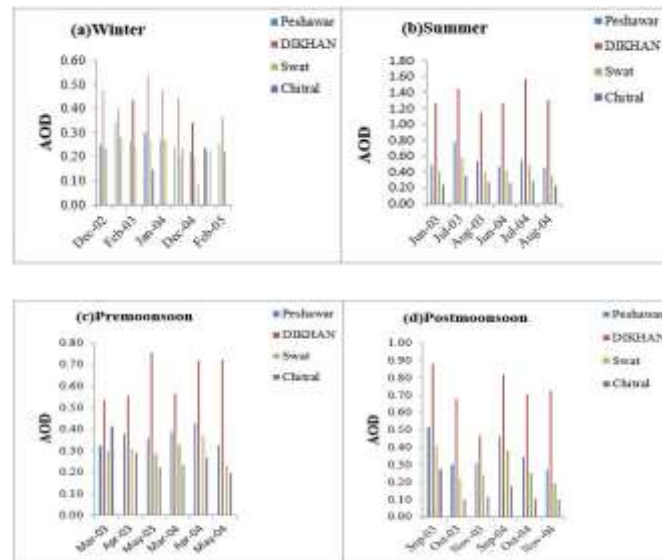


Fig. 3: Seasonal Variations in AOD for winter, summer, pre-monsoon and post-monsoon for the period December 2002 - February 2005 over Peshawar, D I Khan, Swat and Chitral.

3.2 Aerosol radiative forcing (ARF)

3.2.1 Annual and seasonal variation in ARF

The Long Wave (LW) and Short Wave (SW) radiative fluxes at the surface are important components of the Earth's radiation balance (net flow of energy). Thus, the energy fluxes are important to understand climate change, defined by changes in the Earth's energy balance. In this section average ARF was calculated for the LW clear sky at TOA, SRF, and within the atmosphere (ATM) using CERES data. The difference of the two (TOA - SRF) gives ARF within the atmosphere (ATM). The monthly average annual and seasonal ARF variation at TOA, SRF and within the atmosphere (ATM) during clear-sky days for the study period December 2002 - February 2005 were shown in Table 2. The ARF over Peshawar for TOA, SRF and ATM was in the range from 252 to 324 W/m², - 95 to -129W/m² and 349 to 454 W/m², respectively. The ARF over D I Khan for TOA, SRF and ATM was in range of 262-341 W/m², SRF - 62 to -127W/m² and 357-457 W/m², respectively. The monthly mean average clear sky long wave length ARF over Swat for TOA, SRF and ATM was in the range 251-355 W/m², - 80 to -118 W/m² and 347-442 W/m² respectively. The averaged aerosol radiative forcing (ARF) over Chitral for the TOA was 220-305 W/m², while at the surface it was -93 to -122 W/m² leading to an atmospheric forcing of 315-365 W/m². The temporal variations of aerosol forcing in clear sky forcing presented in the figure 4(a-d) that the average forcing in the long wave region within the atmosphere was maximum in the month of June for the years 2003 and 2004 for almost all the cities leading to warming effect. It was noted that the monthly variations of aerosol forcing over studied sites in each year were not uniform. After June the aerosol concentration decreased very slowly due to monsoonal rain resulting in lowest aerosol surface forcing. Likewise, over Chitral AOD was high in September due to anthropogenic forcing at surface and atmosphere. In the long wave region,

interaction of clouds with the long wave radiation leading to increase in the atmospheric forcing (Dey, S. and Tripathi, 2008). In a global study, (Miller et al., 1999) have found that the dust radiative forcing during June–August at the TOA and surface were in the range of -2 to +2 and -5 to -10 W/m². (Alam et al., 2014b) reported longwave ARF values in the range of +6 W/m² and +20W/m² at the earth's surface and +7W/m² and +30W/m² at the TOA producing warming effect in the atmosphere. (Chinnam et al., 2014) also noted heating effect within the atmosphere forcing using LW regions over Kanpur. (Adesina et al., 2014) reported over Gorongosa recorded the monthly mean ARF at TOA, SRF and ATM in the range of -6 to -22 W/m², -16 to -89 W/m² and 10 to 68 W/m², respectively.

Table 2. The average annual and seasonal LW clear sky ARF values retrieved by CERES at the TOA, SRF and within the ATM over Peshawar, D I Khan, Swat and Chitral during the study period.

Sites	ANNUAL			WINTER			SUMMER		
	TOA	SRF	ATM	TOA	SRF	ATM	TOA	SRF	ATM
	W/m ²								
Peshawar	284±23	-108±9	392±30	259±4	-100±4	360±8	313±8	-116±11	429±18
DIKhan	259±23	-104±16	399±30	271±6	-103±6	374±12	321±19	-104±12	425±37
Swat	282±22	-102±11	385±26	258±4	-99±4	358±7	309±10	-106±14	416±21
Chitral	259±26	-105±9	365±35	232±17	-95±2	327±10	284±13	-115±5	399±15

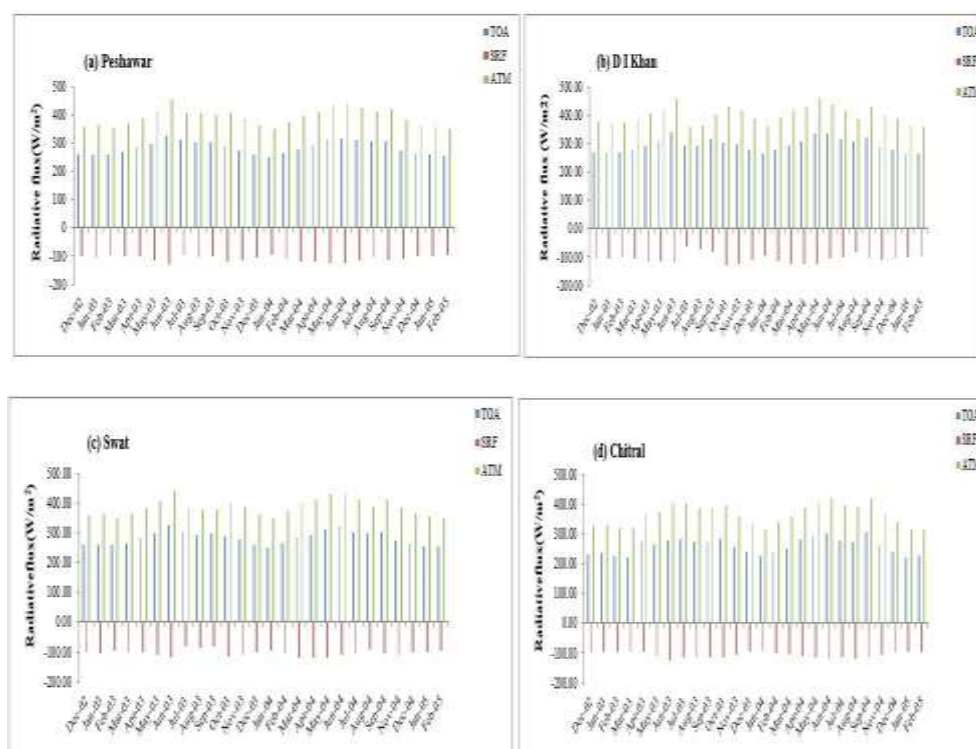


Fig. 4: Monthly averaged variations of radiative forcing (W/m²) at TOA, Surface and within the atmosphere over Peshawar, D I Khan, Swat, Chitral.

(Alam et al., 2011b) over Karachi found that TOA, ATM and SRF was in the range of -7 to -35 W/m², 38 to 61 W/m² and 56 to -96 W/m², respectively. (Ge et al., 2010) noted that surface forcing in the range of -7.9 and -35.8 W/m² over China, which were higher than our values. The global mean clear-sky ARF at the surface was negative found by previous authors (Yu et al., 2006) and (Kim et al., 2008). *Parasad et al.* [48] calculated ARF at SRF between -19 and -87 W/m² and a TOA forcing between +2 and -26 W/m² during over Indo-Gangetic plains (India), which was higher than found in our own study. (Pandithurai, 2008) reported a surface ARF between -39 W/m² (in March) and -99 W/m² (in June), and an atmospheric forcing between +27 W/m² (in March) and +123 W/m² (in June) over New Delhi in 2006. (Prasad et al., 2007) reported that ARF at the surface varied between -45 and -65 W/m² over Morocco, which was higher than the ARF values over Peshawar, D I Khan, Swat and Chitral. (Chinnam et al., 2014) found LW forcing at TOA and surface due to dust were +3 and +2 W/m² respectively. Overall the TOA for Peshawar, D I Khan and Swat were comparable. SRF values were less for D I Khan as compared to the other three location.

Figure 5(a-h) showed the seasonal variation of aerosol radiative flux at TOA, SRF and in the atmosphere over selected sites. Maximum LW ATM flux was found in general in summer, and minimum in winter over all sites. D I Khan and Peshawar show slightly higher values of flux in summer than winter indicating significant heating of the atmosphere and Chitral shows lowest flux in winter. The magnitude of LW ATM flux varied from 315 W/m² in winter over Chitral to 457 W/m² in summer over D I Khan.

The average ARF values found by (Alam et al., 2012) in summer within ATM were 82.6 W/m² and 43.3 W/m² over Lahore and Karachi respectively. Likewise, the average ARF values in winter in ATM were 64.3 W/m² and 41 W/m² over Lahore and Karachi respectively. (Alam et al., 2011b) also reported the same heating effect over Karachi. The large differences between TOA and surface forcing demonstrate that solar radiation is being absorbed within the atmosphere, and as result the atmosphere get warmer but the earth's surface gets cooler (Miller et al., 1999), [45] and (Alam et al., 2011b). This can substantially alter atmospheric stability and influence the dynamic system of the atmosphere (Lee et al., 2010).

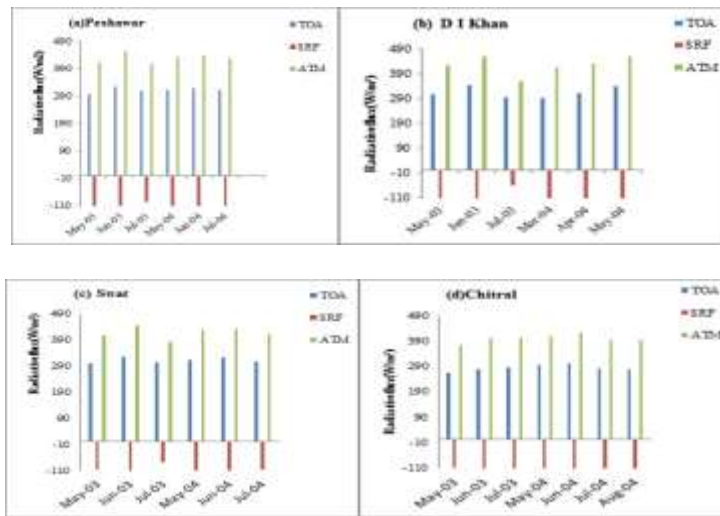
3.3 Intercomparison of MODIS AOD and CERES ARF data

The time series of reflectance anomalies from MODIS and CERES are similar and are well correlated with each other; they are also correlated with the variations of the atmospheric/surface properties, especially cloud fraction, optical depth, and snow/ice coverage. Comparison of AOD measured from MODIS and ARFs of CERES at the SRF, TOA and ATM over Peshawar, D I Khan, Swat and Chitral during the study period was shown in Table 3. The MODIS-retrieved AODs at a wavelength of 550nm compared with CERES-measured at LW ARF at the SRF, TOA and ATM over Peshawar, D I Khan, Swat and Chitral during the study period as shown in figure 6(a-l). The correlation at TOA over Peshawar was found to be relatively high ($R^2=0.58$) between MODISAOD and CERESARF and low ($R^2=0.00$) over Chitral. Therefore, MODISAOD were better matched with CERESARF at the top of the atmosphere over Peshawar.

The correlation at SRF over D I Khan was recorded to be low ($R^2=0.16$) between MODIS AOD and CERES ARF and poor ($R^2=0.01$) between MODIS AOD and CERES ARF over Chitral. Thus MODIS AOD was in reasonable agreement with CERES ARF at the surface over D I Khan. The correlation between MODIS AOD and CERES ARF at ATM was maximum ($R^2=0.48$) over Peshawar and minimum ($R^2=0.02$)

over Chitral, so the good agreement was observed between MODIS retrieved AODs and CERES measured ARF at atmosphere over Peshawar.

SUMMER:



WINTER:

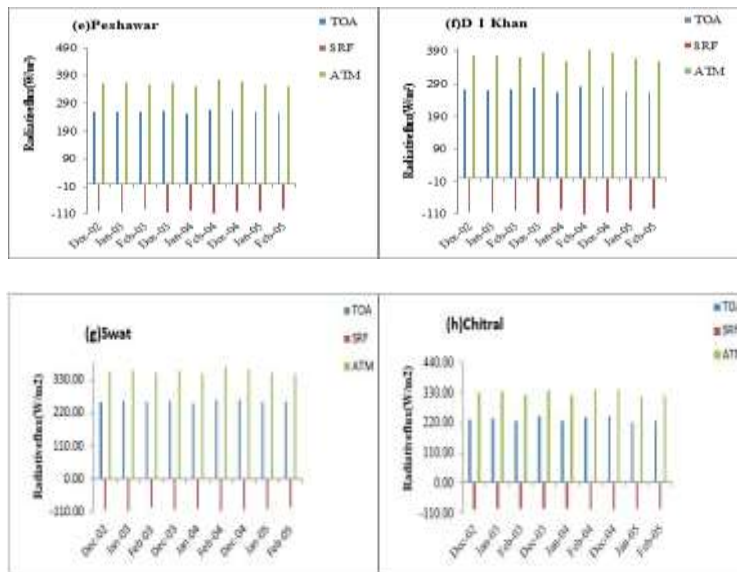
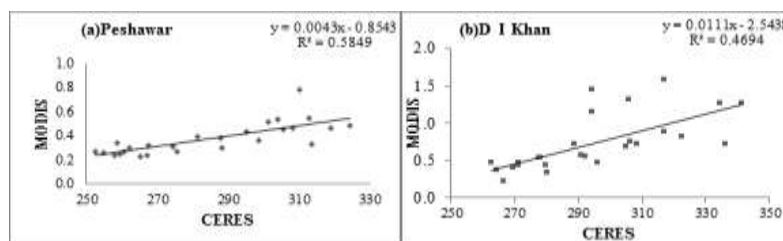
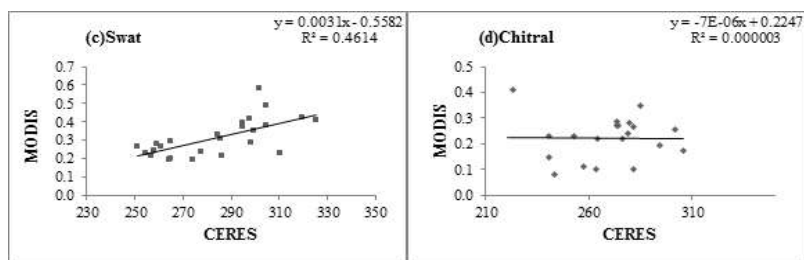


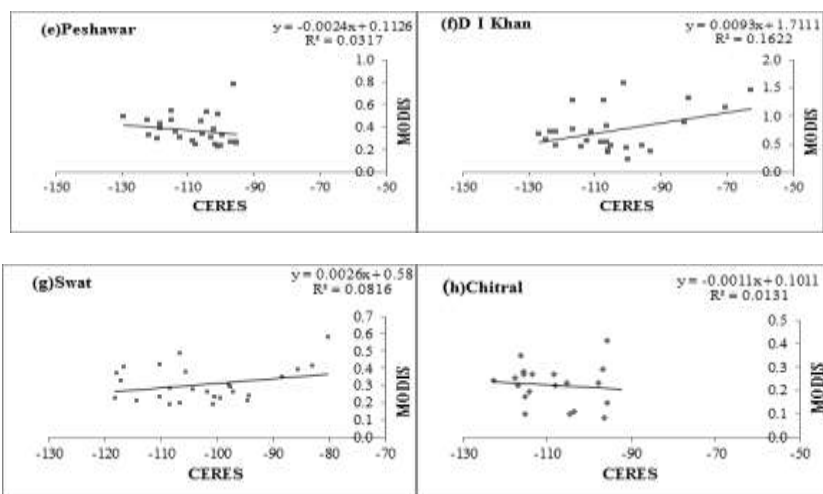
Figure 5. Seasonal variation in aerosol radiative flux over TOA, surface and within the atmosphere over Peshawar, DI Khan, Swat and Chitral for the period (Dec 2002-Feb 2005).

TOA:





SRF:



ATM:

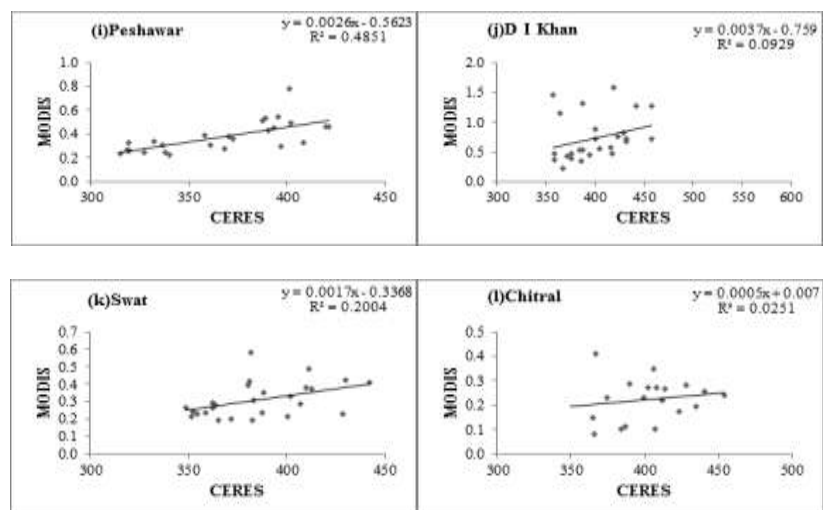


Fig. 6: Intercomparison of MODISAOD and CERESARF (TOA, SRF, and ATM) over Peshawar, D I Khan, Swat and Chitral.

Correlation based on Correlation based on satellites will provide a better understanding of the spatio-temporal behavior of aerosol optical properties and radiative forcing over these sites.

3.4 HYSPLIT trajectories

NOAA HYSPLIT (National Oceanic and Atmospheric Administration Hybrid Single Particle Lagrangian Integrated Trajectory pretends the long-range transport deposition, and scattering, when air masses

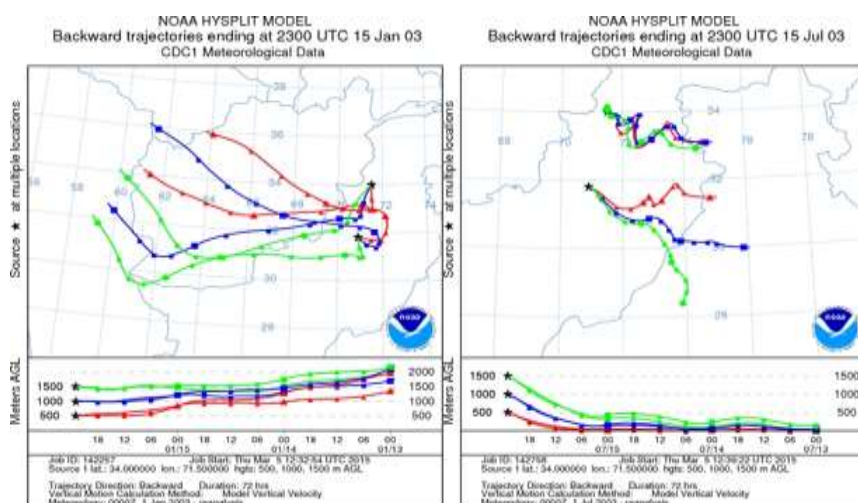
move from the source to the receptors and also measured high and low AODs. Furthermore, with the HYSPLIT model daily back trajectories have been calculated (Draxler et al., 2003) in order to define the origin of the air masses arriving in the area of measurement. There are three main configurations in HYSPLIT, which can be set to characterize the dispersion of the air pollutant (Escudero et al., 2006).

Table 3. Comparison AODs of MODIS and ARFs of CERES and at the TOA, SRF and within the atmosphere over Peshawar, D I Khan, Swat and Chitral during the study period

Sites	MODIS AOD vs CERES ARF		
	TOA (W/m ²)	SRF (W/m ²)	ATM (W/m ²)
	R ²	R ²	R ²
Peshawar	0.58	0.03	0.48
D I Khan	0.47	0.16	0.09
Swat	0.46	0.08	0.20
Chitral	0.000003	0.01	0.02

To investigate the origins of the air masses reaching the studied sites we calculated the three days back long trajectories bringing aerosol particles at three different altitudes above the ground at height of 500m, 1000m and 1500m for 15 January and 15 July 2003. These trajectories are indicative of the study period analyzed.

Figure.7 depicted the probable transport of air masses from the source area to Peshawar, D I Khan, Swat and Chitral from the Iran, the Turkmenistan, India and Afghanistan also some air masses were from Baluchistan Punjab and Azad Kashmir. Anthropogenic aerosol sources (fine aerosols from the burning of fossil fuels and biomass, industrial activity, cooking and traffic) contributed to an increase in aerosol concentrations over different sites in Pakistan (Alam et al., 2011a).



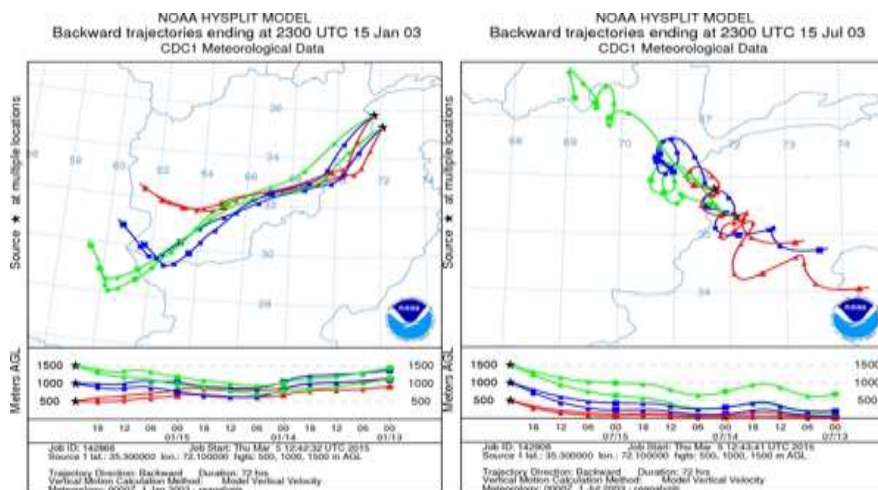


Fig. 7: Three-day back-trajectories representing the air mass at three different heights reaching Peshawar, D I Khan, Swat and Chitral on a specific day in the month of January 2003 and July 2003.

Conclusion

This paper emphasizes on the annual and seasonal variations of monthly mean AOD values from MODIS and aerosol optical and radiative forcing from CERES data for the period of December 2002 - February 2005 over Peshawar, D I Khan, Swat and Chitral.

The major conclusions of the study are:

1. Highest average AODs were observed over D I Khan (0.73); while the lowest AODs were found over Chitral (0.22). AODs over Peshawar (0.37) and Swat (0.31) were relatively higher but then Highest AODs over D I Khan occur as the location is hot desert with hot summers and mild winters and Precipitation could contribute additionally to the increase in AODs.
2. Over the study locations change in AODs is observed due to seasonal variation because of wind speeds, relative humidity, and temperature changes.
3. Using CERES data, we analyzed the clear-sky long-wave aerosol radiative forcing at top of the atmosphere and at surface to compute atmospheric forcing which leads to warming of the atmosphere data.
4. The MODIS-retrieved AODs compared with CERES-measured at LW ARF at the SRF, TOA and ATM over all sites and found best correlation ($R^2 = 0.58$) between MODIS AODs and CERES ARF over Peshawar than other sites.
5. We also used the Hybrid Single Particle Lagrangian Integrated Trajectory (HYSPLIT) model to analyze trajectories of air masses, in order to understand the spatial-temporal variation in aerosol loading.

Acknowledgement

The authors are thankful to the MODIS (<http://modis.gsfc.nasa.gov/>) teams at NASA for the providing AOD data, NASA and managed by NASA's Langley Research Center (LaRC) in Hampton, Virginia for providing CERES data (<http://ceres.larc.nasa.gov/>). The authors are also grateful to the

NOAA Air Resources Laboratory (ARL) for the provision of the HYSPLIT transport and dispersion model (<http://www.arl.noaa.gov/ready.html>) used in this publication.

References

- [1] Fu, Q., Lesins, G., Higgins, J. and Michalsky, J. 1999. Aerosol direct radiative forcing: A five year climatology at the ARM SGP CART site. Ninth ARM Science Team Meeting, San Antonio, Tex.
- [2] Pollack, H. N., Hurter, S. J. and Johnson, J. R., 1993. Heat flow from the Earth's interior: analysis of the global data set. *Reviews of Geophysics* 313: 267-280.
- [3] Pawar, G., Devara, P., More, S., Kumar, P. P. and Aher, G., 2012. Determination of aerosol characteristics and direct radiative forcing at Pune. *Aerosol Air Qual. Res* 12: 1166-1180.
- [4] Russell, P. B., Hobbs, P. V. and Stowe, L. L., 1999. Aerosol properties and radiative effects in the United States east coast haze plume: An overview of the Tropospheric Aerosol Radiative Forcing Observational Experiment (TARFOX). *Journal of Geophysical Research: Atmospheres* (1984–2012) 104D2: 2213-2222.
- [5] Kratz, D. P., Gupta, S. K., Wilber, A. C. and Sothcott, V. E., 2010. Validation of the CERES Edition 2B surface-only flux algorithms. *Journal of Applied Meteorology and Climatology* 491: 164-180.
- [6] Satheesh, S. and Ramanathan, V., 2000. Large differences in tropical aerosol forcing at the top of the atmosphere and Earth's surface. *Nature* 4056782: 60-63.
- [7] Chou, C., Neelin, J. D., Lohmann, U. and Feichter, J., 2005. Local and Remote Impacts of Aerosol Climate Forcing on Tropical Precipitation*. *Journal of climate* 1822: 4621-4636.
- [8] Griggs, D. J. and Noguer, M., 2002. Climate change 2001: the scientific basis. Contribution of working group I to the third assessment report of the intergovernmental panel on climate change. *Weather* 578: 267-269.
- [9] Chung, C. E., Ramanathan, V., Kim, D. and Podgorny, I., 2005. Global anthropogenic aerosol direct forcing derived from satellite and ground-based observations. *Journal of Geophysical Research: Atmospheres* (1984–2012) 110D24.
- [10] Chakraborty, A., Satheesh, S., Nanjundiah, R. and Srinivasan, J. 2004. Impact of absorbing aerosols on the simulation of climate over the Indian region in an atmospheric general circulation model. *Annales geophysicae, Copernicus Group*.
- [11] Alam, K., Trautmann, T. and Blaschke, T., 2011b. Aerosol optical properties and radiative forcing over mega-city Karachi. *Atmospheric Research* 1013: 773-782.
- [12] Pandithurai, G., Dipu, S., Dani, K., Tiwari, S., Bisht, D., Devara, P. and Pinker, R., 2008. Aerosol radiative forcing during dust events over New Delhi, India. *Journal of Geophysical Research: Atmospheres* (1984–2012) 113D13.
- [13] Collins, W. D., Rasch, P. J., Eaton, B. E., Fillmore, D. W., Kiehl, J. T., Beck, C. T. and Zender, C. S., 2002. Simulation of aerosol distributions and radiative forcing for INDOEX: Regional climate impacts. *Journal of Geophysical Research: Atmospheres* (1984–2012) 107D19: INX2 27-21-INX22 27-20.
- [14] Qin, J., Yang, K., Liang, S. and Guo, X., 2009. The altitudinal dependence of recent rapid warming over the Tibetan Plateau. *Climatic Change* 971-2: 321-327.
- [15] Deepshikha, S., Satheesh, S. and Srinivasan, J., 2005. Regional distribution of absorbing efficiency of dust aerosols over India and adjacent continents inferred using satellite remote sensing. *Geophysical research letters* 323.
- [16] Menon, S., Hansen, J., Nazarenko, L. and Luo, Y., 2002. Climate effects of black carbon aerosols in China and India. *Science* 2975590: 2250-2253.
- [17] Zhang, H., Wang, Z., Guo, P. and Wang, Z., 2009. A modeling study of the effects of direct radiative forcing due to carbonaceous aerosol on the climate in East Asia. *Advances in atmospheric sciences* 26: 57-66.
- [18] Alam, K., Iqbal, M. J., Blaschke, T., Qureshi, S. and Khan, G., 2010. Monitoring spatio-temporal variations in aerosols and aerosol–cloud interactions over Pakistan using MODIS data. *Advances in Space Research* 469: 1162-1176.
- [19] Tanré, D., Kaufman, Y., Herman, M. and Mattoo, S., 1997. Remote sensing of aerosol properties over oceans using the MODIS/EOS spectral radiances. *Journal of Geophysical Research: Atmospheres* (1984–2012) 102D14: 16971-16988.
- [20] Kaufman Y. J., Remer L. A., Tanré D., Li, R. R., Kleidman R., Mattoo, S., Levy, R. C., Eck, T. F., Holben, B. N. and Ichoku, C., 2005. A critical examination of the residual cloud contamination and diurnal sampling effects on MODIS estimates of aerosol over ocean. *Geoscience and Remote Sensing, IEEE Transactions on* 4312: 2886-2897.

- [21] Remer L. A., Kaufman Y. Tanré D., Mattoo S., Chu D., Martins J. V., Li R. R., Ichoku C., Levy R. and Kleidman R., 2005, The MODIS aerosol algorithm, products, and validation. *Journal of the atmospheric sciences* 62, 947-973.
- [22] Loeb N. G., Manalo-Smith N., Kato S., Miller W. F., Gupta S. K., Minnis P. and Wielicki B. A., 2003, Angular distribution models for top-of-atmosphere radiative flux estimation from the Clouds and the Earth's Radiant Energy System instrument on the Tropical Rainfall Measuring Mission Satellite. Part I: Methodology. *Journal of applied meteorology*, 42, 240-265.
- [23] Draxler R. and Rolph G., 2003, HYSPLIT (HYbrid Single-Particle Lagrangian Integrated Trajectory). NOAA Air Resources Laboratory, Silver Spring, MD. Model access via NOAA ARL READY Website.
- [24] Jin M., 2006, MODIS observed seasonal and interannual variations of atmospheric conditions associated with hydrological cycle over Tibetan Plateau. *Geophysical research letters*, 3319.
- [25] Sarkar S., Chokngamwong R., Cervone G., Singh R. and Kafatos M., 2006, Variability of aerosol optical depth and aerosol forcing over India. *Advances in Space Research*, 3712, 2153-2159.
- [26] El-Metwally M., Alfaro S., Wahab M. A., Zakey A. and Chatenet, B., 2010, Seasonal and inter-annual variability of the aerosol content in Cairo (Egypt) as deduced from the comparison of MODIS aerosol retrievals with direct AERONET measurements. *Atmospheric Research*, 971, 14-25.
- [27] Ranjan R. R., Joshi H. and Iyer K., 2007, Spectral variation of total column aerosol optical depth over Rajkot: a tropical semi-arid Indian station. *Aerosol Air Qual. Res*, 71, 33-45.
- [28] Balakrishnaiah G., Reddy B. S. K., Gopal K. R., Reddy R., Reddy L., Swamulu C., Ahammed Y. N., Narasimhulu K., KrishnaMoorthy K. and Babu S. S., 2012, Spatio-temporal variations in aerosol optical and cloud parameters over Southern India retrieved from MODIS satellite data. *Atmospheric Environment*, 47, 435-445.
- [29] Tripathi S., Dey S., Chandel A., Srivastava S., Singh R. P. and Holben B. 2005, Comparison of MODIS and AERONET derived aerosol optical depth over the Ganga Basin, India, *Annales Geophysicae*.
- [30] Li C., Mao J., Lau K. H. A., Chen J. C., Yuan Z., Liu X., Zhu A. and Liu G., 2003, Characteristics of distribution and seasonal variation of aerosol optical depth in eastern China with MODIS products. *Chinese Science Bulletin*, 4822, 2488-2495.
- [31] Wang Y., Xin J., Li Z., Wang S., Wang P., Hao W., Nordgren B., Chen H., Wang L. and Sun Y., 2008, Seasonal variations in aerosol optical properties over China. *Atmospheric Chemistry and Physics Discussions* 83, 8431-8453.
- [32] Papadimas C., Hatzianastassiou N., Mihalopoulos N., Querol X. and Vardavas I., 2008, Spatial and temporal variability in aerosol properties over the Mediterranean basin based on 6-year (2000–2006) MODIS data. *Journal of Geophysical Research: Atmospheres (1984–2012)* 113D11.
- [33] Chen D. and Tian J. 2010, Monitoring spatial and temporal variability of air quality using satellite observation data: A case study of MODIS-observed aerosols in Southern Ontario, Canada, INTECH Open Access Publisher.
- [34] Singh S., Soni, K., Bano, T., Tanwar, R., Nath, S. and Arya, B. 2010. Clear-sky direct aerosol radiative forcing variations over mega-city Delhi. *Annales Geophysicae*, Copernicus GmbH.
- [35] Alam K., Sahar, N. and Iqbal, Y., 2014a. Aerosol characteristics and radiative forcing during pre-monsoon and post-monsoon seasons in an urban environment. *Aerosol Air Qual. Res* 141: 99-107.
- [36] Choudhry, P., Misra, A. and Tripathi, S. 2012. Study of MODIS derived AOD at three different locations in the Indo Gangetic Plain: Kanpur, Gandhi College and Nainital. *Annales Geophysicae*, Copernicus GmbH.
- [37] Kalita G. and Bhuyan, P. K., 2011. Spatial heterogeneity in tropospheric ozone over the Indian subcontinent: long-term climatology and possible association with natural and anthropogenic activities. *Advances in Meteorology*, 924516, doi.org/10.1155/2011/924516.
- [38] Pathak B., Bhuyan, P. K., Biswas J., Takemura T., 2013, Long term climatology of particulate matter and associated microphysical and optical properties over Dibrugarh, North–EastIndia and inter-comparison with SPRINTARS simulations. *Atmospheric Environment*, 69, 334-344.
- [39] Kharol K. S., Badarinath K.V.S., Roy P. S., 2008, Studies on emission from forest fires using multi-satellite datasets over north east region of India. *The International Archives of the Photogrammetry. Geoscience and Remote Sensing*, Beijing.
- [40] Dey S. and Tripathi S., 2008, Aerosol direct radiative effects over Kanpur in the Indo-Gangetic basin, northern India: Long-term (2001–2005) observations and implications to regional climate. *Journal of Geophysical Research: Atmospheres (1984–2012)* 113D4.
- [41] Miller R. and Tegen I., 1999, Radiative forcing of a tropical direct circulation by soil dust aerosols. *Journal of the atmospheric sciences*, 5614, 2403-2433.

- [42] Alam K., Trautmann T., Blaschke T. and Subhan F., 2014b, Changes in aerosol optical properties due to dust storms in the Middle East and Southwest Asia, *Remote Sensing of Environment*, 143, 216-227.
- [43] Chinnam N., Dey S., Tripathi S. and Sharma M., 2006, Dust events in Kanpur, northern India, Chemical evidence for source and implications to radiative forcing, *Geophysical Research Letters*, 338.
- [44] Adesina A. J., Kumar, K. R. and Sivakumar, V., 2014, Variability in aerosol optical properties and radiative forcing over Gorongosa (18.97° S, 34.35° E) in Mozambique, *Meteorology and Atmospheric Physics*, 1-12.
- [45] Ge J., Su J., Ackerman T., Fu Q., Huang J. and Shi J., 2010, Dust aerosol optical properties retrieval and radiative forcing over northwestern China during the 2008 China-US joint field experiment, *Journal of Geophysical Research, Atmospheres (1984–2012)* 115D7.
- [46] Yu X., Cheng T., Chen J. and Liu Y., 2006, A comparison of dust properties between China continent and Korea, Japan in East Asia. *Atmospheric Environment*, 4030, 5787-5797.
- [47] Kim D. and Ramanathan V., 2008, Solar radiation budget and radiative forcing due to aerosols and clouds, *Journal of Geophysical Research, Atmospheres (1984–2012)* 113D2.
- [48] Prasad A. K., Singh S., Chauhan S., Srivastava M. K., Singh R. P. and Singh R., 2007, Aerosol radiative forcing over the Indo-Gangetic plains during major dust storms, *Atmospheric Environment*, 4129, 6289-6301.
- [49] Bierwirth E., Wendisch M., Ehrlich A., Heese B., Tesche M., Althausen D., Schladitz A., Müller D., Otto S. and Trautmann, T., 2009. Spectral surface albedo over Morocco and its impact on radiative forcing of Saharan dust, *Tellus B* 611, 252-269.
- [50] Alam K., Trautmann, T., Blaschke T. and Majid H., 2012, Aerosol optical and radiative properties during summer and winter seasons over Lahore and Karachi. *Atmospheric Environment* 50: 234-245.
- [51] Li Z., Lee, K. H., Wang, Y., Xin J. and Hao W. M., 2010, First observation-based estimates of cloud-free aerosol radiative forcing across China. *Journal of Geophysical Research: Atmospheres (1984–2012)* 115D7.
- [52] Escudero M., Stein, A., Draxler R., Querol X., Alastuey A., Castillo S. and Avila A., 2006, Determination of the contribution of northern Africa dust source areas to PM10 concentrations over the central Iberian Peninsula using the Hybrid Single-Particle Lagrangian Integrated Trajectory model (HYSPLIT) model. *Journal of Geophysical Research, Atmospheres (1984–2012)* 111D6.
- [53] Alam K., Blaschke T., Madl P., Mukhtar A., Hussain M., Trautmann T. and Rahman S., 2011a, Aerosol size distribution and mass concentration measurements in various cities of Pakistan, *Journal of Environmental Monitoring* 137, 1944-1952.